Density functional study of Au_nCu (n = 1–7) clusters*

Guo Jian-Jun(郭建军)[a)†], Wei Cheng-Fu(魏成富)[b)],
Yang Ji-Xian(杨继先)[a)], and Die Dong (迭 东)[a)]

[a)] *School of Physics and Chemistry, Xihua University, Chengdu* 610039, *China*
[b)] *Mianyang Normal University, Mianyang* 621000, *China*

(Received 12 March 2010; revised manuscript received 26 April 2010)

The possible stable geometrical configurations and the relative stabilities of the lowest-lying isomers of copper-doped gold clusters, Au_nCu (n = 1–7), are investigated using the density functional theory. Several low-lying isomers are determined. The results indicate that the ground-state Au_nCu clusters have planar structures for n = 1–7. The stability trend of the Au_nCu clusters (n = 1–7), shows that odd-numbered Au_nCu clusters are more stable than the neighbouring even-numbered ones, thereby indicating the Au_5Cu clusters are magic cluster with high chemical stability.

Keywords: density functional theory, Au–Cu clusters, structure, stability
PACC: 3640, 3640B, 3120A, 3130J

1. Introduction

Transition bimetal clusters continue to be an important object of investigation due to their wide range of applications.[1−7] This is motivated by the fact that a transition metal atom doped in a small cluster of other metal can strongly change the properties of the host cluster. A great number of investigations have been performed on heteroatomic or impurity-doped as well as homoatomic metal clusters, which indicate that the impurity atoms can strongly influence geometric, electronic, and bonding properties of mixed clusters.[8−11] Most theoretical and experimental studies of bimetallic clusters focus on single-impurity alkali-metal clusters to examine the jellium model and to clarify bonding characteristics between impurity atoms and host clusters.[12−16]

Recently, the noble-metal (Cu, Ag, and Au) clusters have aroused considerable interest of chemists and physicists due to their unique physical and chemical properties.[17−22] For example, Bouwen *et al.*[23] and Heinebrodt *et al.*[24] investigated the bimetallic $Au_nX_m^+$ clusters (X = Cu, Al, Y, In, Cs). Binary Au cluster anions with a doped metal atom: Au_nM^- (n = 2–7), M = Pd, Ni, Zn, Cu, and Mg, were investigated using anion photoelectron spectroscopy by Koyasu *et al.*[5] Yuan *et al.*[12] investigated the geometric, electronic, and bonding properties of Au_nM (n = 1–7, M = Ni, Pd, Pt) clusters. The geometric structures, relative stabilities, and magnetic moments of the small Au_nFe (n =1–7) clusters have been investigated systematically by density functional theory (DFT) in Ref. [1]. Nonlinear optical properties of $Au_{n-m}M_m$ (M = Ag, Cu; m = 1, 2) clusters were theoretically investigated.[6] The results show that the second metal atom doped in clusters of Au atoms plays a special role in their stabilities and chemical activities.

In the present paper, we systematically investigate the geometric structures and the stability trend of Au_nCu (n = 1–7) clusters using the *ab initio* method based on DFT. Effective core potentials (ECP) including relativistic effects (RECP) for the gold and copper atoms are introduced in order to describe the inner core electrons. Our main objective is to determine the possible stable geometrical structures with their electronic states of binary Au_nCu (n = 1–7) clusters, and investigate the stability trend.

The remainder of the present paper is organised as follows. In Section 2, we briefly describe our theoretical approach. The geometries of the lowest-lying isomers of Au_nCu (n = 1–7) clusters are given in Section 3, and the stability trend is investigated in Section 4. Section 5 contains a summary of our results.

2. Computational methods

In the present calculation, geometry optimizations and vibrational frequency analyses are carried using DFT with the unrestricted B3LYP exchange–

*Project supported by the Foundation from the Education Commission of Sichuan Province, China (Grant No. 2006B042).
†Corresponding author. E-mail: jmst_gjj@163.com
© 2010 Chinese Physical Society and IOP Publishing Ltd

correlation functional and an effective core potential LANL2DZ basis set[25−27] as implemented in GAUSSIAN03 program package.[28] To search the lowest energy structures of Au_nCu (n = 1–7) clusters, lots of possible initial configurations, which have different bond lengths, bond angles, or point groups, are used in geometry optimizations. Furthermore, the previous studies on gold clusters are also employed as a guide.[18] Due to the spin polarisation, each initial configuration is optimized at various possible spin multiplicities. Each geometry optimization is followed by a calculation of harmonic vibrational frequencies to confirm that the optimized geometry corresponds to a local minimum. In all calculations, the convergence thresholds are set to be 0.000015 Hartree/Bohr (1 Hartree = 27.21 eV) for the force, 0.000060 Å (1 Å = 0.1 nm) for the displacement, and 10^{-6} Hartree for the energy change.

The accuracy of the computational method is checked by calculations of Cu_2, Au_2 and AuCu dimers. The calculated total energy E, equilibrium distance r_e, molecular state, vibrational frequency ω_e and dissociation energy D_e for the ground states of Cu_2, Au_2 and AuCu clusters are given in Table 1 together with the experimental values. Our results are very close to the experimental values. Satisfactory agreement indicates that our choice of density functional, effective core potential including relativistic effects, and basis set used in current density functional calculations should be good to describe the Au_nCu (n = 1–7) clusters.

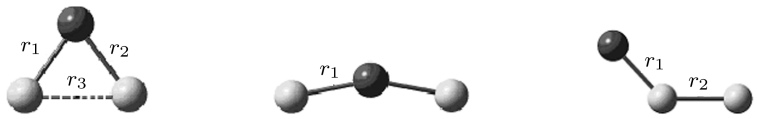
Table 1. Properties of Cu_2, Au_2, and AuCu using B3LYP with LANL2DZ basis set.

cluster	state	E/arb. units	r_e/Å	ω_e/cm^{-1}	D_e/eV	dipole moment/Debye
Cu_2	$^1\Sigma_g^+$	–392.30768	2.26(2.22)[a]	256(266)	2.02(2.01)	
Au_2	$^1\Sigma_g^+$	–270.94842	2.57(2.47)[b]	180(191)	1.88(1.88)	
AuCu	$^1\Sigma^+$	–331.64093	2.40(2.33)[c]	230(248)	2.29(2.34)	2.6291

[a] Experimental values of Cu_2 in parentheses see Ref. [29]. [b] Experimental values of Au_2 in parentheses see Ref. [30].
[c] Experimental values of AuCu in parentheses see Ref. [31].

3. Geometrical configurations

Figure 1 and Table 2 show the optimized results of the Au_2Cu cluster. The most stable structure of Au_2Cu is a triangular C_s configuration in the $^2A'$ electronic state (I_1), which shows relaxed Au–Cu and Au–Au distances with respect to the AuCu and Au_2 dimers equilibrium distances as compared with that calculated for the AuCu and Au_2 dimers in Table 1. These structural changes already reflect the degree of distortion that the impurity atom can produce for the geometry of bare metallic cluster. The triangular structure in the $^2B_2$ electronic state is next in energy, which has C_{2v} symmetry with an apex angle of 154.16°. The triangular C_s configuration with the Cu–Cu bond (I_3) is 0.35 eV higher in energy than the lowest energy form.



I_1 I_2 I_3

Fig. 1. Stable structures of Au_2Cu, where Cu atoms are denoted as darker spheres. The values of distance r_i are given in Table 2.

Table 2. Properties of the Au_2Cu cluster: geometry, molecular state and point group, relative energy, binding energy per atom (E_b) and dipole moment for isomer I_1, and vibrational frequency (bold figures are frequencies of the most IR-intense mode).

geometry $r_1/r_2.../$Å	state/group	total energy (arb. units)/I_1 (eV)	E_b/eV	dipole moment/Debye	frequency/cm^{-1}
I_1: 2.50/2.49/2.91	$^2A'/C_s$	–467.12363/0.00	1.15	2.4874	66,147,**213**
I_2: 2.47	$^2B_2/C_{2v}$	–467.11672/0.19			13,110,**234**
I_3: 2.45/2.66	$^2A'/C_s$	–467.11082/0.35			22,**124**,198

The trial geometries used in the geometry optimizations of the Au_3Cu cluster are the isomers of the Au_4 cluster.[18] In addition, we also consider the linear configurations. The calculated stable structures are shown in Fig. 2, and their properties are listed in Table 3. Four isomers of Au_3Cu have been found by geometry optimization, which include geometries of different spin multiplicities. The rhombus structure with C_{2v} symmetry in the $^1A_1$ electronic state is the most stable isomer as it also occurred in the Au_4 cluster optimizations.[18] The T-form (isomer I_2) is next in energy. Isomer I_3 with a similar structure is 1.15 eV higher in energy than isomer I_1. The structure of highest energy is a three-dimensional (3D) structure with C_{3v} symmetry in the $^5A_1$ electronic state. Transition from two-dimensional (2D) to three-dimensional (2D→3D) structures occurs from isomer I_3 to isomer I_4, with an energy change of 3.24 eV. This result is disagreement with the Au_4 cluster sequence where the rhombus-to-tetrahedral transition occurred with an energy change of ∼1.00 eV.[18] Comparing the energy difference between isomers I_1 and I_2 of Au_3Cu cluster with those of the same sequences of the Au_4 cluster,[18] it is found that one Cu atom incorporated in the Au_4 cluster increase the energy difference by 0.8 eV.



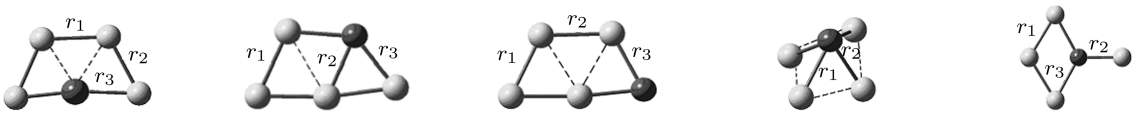
I_1 I_2 I_3 I_4

Fig. 2. Stable structures of Au_3Cu, where Cu atoms are represented as darker spheres. The values of distance r_i are reported in Table 3.

Table 3. Properties of the Au_3Cu cluster: geometry, molecular state and point group, relative energy, binding energy per atom (E_b) and dipole moment for isomer I_1, and vibrational frequency (bold figures are the frequencies of the most IR-intense mode).

geometry $r_1/r_2\ldots$/Å	state/group	total energy (arb. units)/I_1 (eV)	E_b/eV	dipole moment /Debye	frequency/cm^{-1}
I_1: 2.61/2.52/2.73	$^1A_1/C_{2v}$	–602.64416/0.00	1.41	1.0519	38,67,99,104,**174**,201
I_2: 2.42/2.89/2.61	$^1A_1/C_{2v}$	–602.61245/0.86			10,**33**,56,74,155,221
I_3: 2.53/2.75	$^3B_2/C_{2v}$	–602.60185/1.15			15,30,95,121,**154**,186
I_4: 2.648	$^5A_1/C_{3v}$	–602.48274/4.39			**37**,38,87,94,166

Figure 3 and Table 4 show the stable isomers and properties of the Au_4Cu cluster. The most stable structure is planar trapezoidal structure with impurity centred in the middle of bottom lateral as it also occurs in the Au_4Fe cluster optimizations.[1] This structure has a binding energy of 1.45 eV per atom, which is higher than those for the structures I_2 and I_3. Isomer I_3, of which the impurity atom occupies apex position, is found at an energy of 0.56 eV above that of the ground state structure. The first 2D→3D transition occurs in isomer I_3, which is 0.20 eV lower in energy than the equivalent first 3D isomer of the Au_5 cluster.[18] A higher energy 3D structure with the Cu atom occupying the apex position (I_4) is also found in our calculation. Isomer I_5 with the impurity atom occupying the central position has a planar structure, which is 0.83 eV higher in energy than the isomer I_1. This geometry might be well described as perturbations to the most stable rhombic structure of the Au_3Cu cluster by the addition of one Au atom. We also optimize the Cu-centred Au_4 rhombus, the ground-state form of Au_5Cu reported in Ref. [21], obtaining a saddle point, 1.43 eV in energy higher than the ground state.



I_1 I_2 I_3 I_4 I_5

Fig. 3. Stable structures of Au_4Cu, where Cu atoms are denoted as dark spheres and the values of distance r_i are given in Table 4.

Table 4. Properties of Au_4Cu cluster: geometry, molecular state and point group, relative energy, binding energy per atom (E_b) and dipole moment for isomer I_1, and vibrational frequency (bold figures are the frequencies of the most IR-intense mode).

geometry $r_1/r_2\ldots$/Å	state/group	total energy (arb. units)/I_1 (eV)	E_b/eV	dipole moment /Debye	frequency/cm^{-1}
I_1:2.77/2.72/2.56	$^2A_1/C_{2v}$	–738.14276/0.00	1.45	0.2179	21,43,52,64,89,107,129,154,**224**
I_2:2.79/2.60/2.58	$^2A'/C_s$	–738.13808/0.13			26,35,43,69,89,101,149,171,**197**
I_3:2.73/2.82/2.57	$^2A'/C_s$	–738.12189/0.56			23,32,46,59,92,107,120,**144**,199
I_4:2.63/2.57	$^2B_1/C_{2v}$	–738.12011/0.61			19,25,49,65,70,91,143,155,**193**
I_5:2.69/2.41/2.61	$^2B_2/C_{2v}$	–738.11224/0.83			15,41,46,53,64,122,160,173,**252**

The stable isomers of the Au_5Cu cluster are depicted in Fig. 4, and their properties are reported in Table 5. The lowest-energy structure corresponds to a planar triangular configuration with impurity centred in the middle of bottom lateral (I_1). This geometry is also the most stable isomer in the Au_6 cluster.[18] The triangular structure with the Cu atom at the outmost position (I_3) is 0.62 eV less in energy than the ground state configuration. Isomers I_2 and I_4 are 3D forms, which have energies higher than isomer I_1. However, isomer I_2 was the most stable isomer of Au_5Cu reported in Ref. [21]. Looking at the energy differences between isomers I_1, I_2, and I_4, it is found that they are disagreement with those obtained for the Au_6 cluster. In particular, the difference in energy between isomer I_2 and isomer I_1 is 0.49 eV for both sequences.[18] Several low-lying isomers of the Au_6 cluster do not remain at local minima for the Au_5Cu cluster.



I_1 I_2 I_3 I_4

Fig. 4. Stable structures of Au_5Cu, where Cu atoms are denoted as dark spheres and the values of distance r_i are given in Table 5.

Table 5. Properties of Au_5Cu cluster: geometry, molecular state and point group, relative energy, binding energy per atom (E_b) and dipole moment for isomer I_1, and vibrational frequency. (bold figures are the frequencies of the most IR-intense mode.)

geometry $r_1/r_2\ldots$/Å	state/group	total energy (arb. units)/I_1 (eV)	E_b/eV	dipole moment /Debye	frequency/cm^{-1}
I_1:2.70/2.67/2.57	$^1A_1/C_{2v}$	–873.67713/0.00	1.64	0.4588	32,34,43,59,61,68,79,110,138,141,172,**226**
I_2:2.58	^{1}A'/C_s	-873.66132/0.43			23,24,50,70,72,80,81,143,213,**214**
I_3:2.55/2.73/2.69	$^1A_1/C_{2v}$	–873.65417/0.62			31,35,46,59,79,90,109,122,132,**165**,205
I_4:2.90/3.07/2.63	$^5A_2/C_{2v}$	–873.54445/3.61			33,42,45,46,54,77,95,143,**158**

The stable isomers of the Au_6Cu cluster are depicted in Fig. 5, and their properties are indicated in Table 6. Due to the stable capped triangle structure of Au_7,[18] seven planar capped triangles (I_1, I_2, I_3, I_4, I_5, I_6, and I_7) each with C_s symmetry in the ^2A' electronic state have been found by optimizations, which may originate from one Cu atom substitution in the lowest energy structure of Au_7.[18] Among them, isomer I_1 is the most stable triangular structure. This structure (I_1) has a binding energy of 1.56 eV per atom, which is higher than that for the similar structures (I_2, I_3, I_4, I_5, I_6, and I_7). Isomer I_8 is an extended W form as it also occurs in the Au_7 cluster optimization.[18] Isomer I_9 is of a hexagon with the Cu atom occupying the centre of the ring, which is 1.88 eV higher in energy than the isomer I_1. The 3D isomers of the Au_7 cluster[18] and the ground state structure of Au_6Cu cluster reported in Ref. [21] do not remain at local minima for the Au_6Cu cluster. Moreover, the ground state structure of Au_7 clusters investigated by Wang *et al.*[21] is not consistent with the theoretical ones reported in Ref. [18], either.

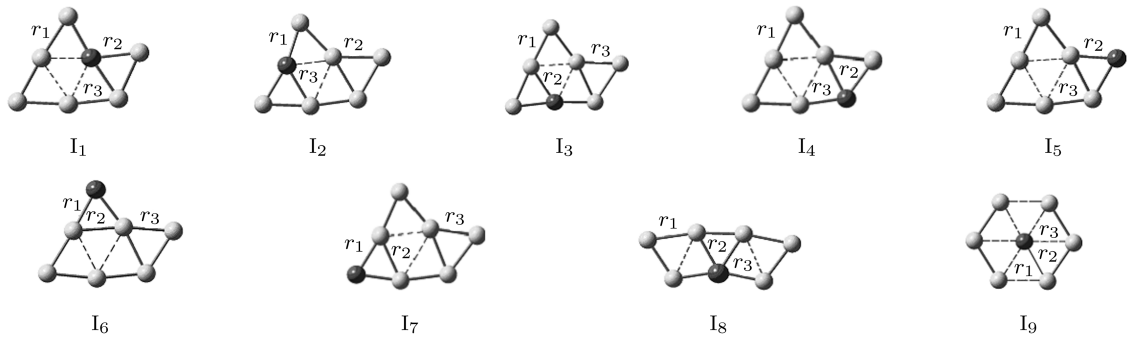


Fig. 5. Stable structures of Au_6Cu, where Cu atoms are denoted as darker spheres. The values of distance r_i are reported in Table 6.

Table 6. Properties of Au_6Cu cluster: geometry, molecular state and point group, relative energy, binding energy per atom (E_b) and dipole moment for isomer I_1, and vibrational frequency. (bold figures are frequencies of the most IR-intense mode.)

geometry $r_1/r_2\ldots$/Å	state/group	total energy (arb. units)/I_1 (eV)	E_b/eV	dipole moment /Debye	frequency/cm^{-1}
I_1:2.66/2.60/2.70	^{2}A'/C_s	–1009.15782/0.00	1.56	0.1188	10,28,33,35,46,48,57,74,79,104,108,138,159,166,**223**
I_2:2.55/2.78/2.65	^{2}A'/C_s	–1009.15495/0.08			11,27,32,35,43,48,60,66,80,102,112,134,147,162,**230**
I_3:2.69/2.66/2.74	^{2}A'/C_s	–1009.15193/0.16			11,33,35,37,40,49,59,73,85,97,107,130,145,172,**223**
I_4:2.68/2.55/2.56	^{2}A'/C_s	–1009.14690/0.30			15,28,31,33,36,46,58,76,85,99,109,126,**165**,178,200
I_5:2.71/2.56/2.73	^{2}A'/C_s	–1009.13614/0.59			15,28,33,35,52,62,71,86,103,110,117,148,**163**,191
I_6:2.54/2.74/2.74	^{2}A'/C_s	–1009.13597/0.59			13,24,26,35,36,49,62,74,80,105,110,128,144,**154**,210
I_7:2.55/2.77/2.75	^{2}A'/C_s	–1009.13395/0.65			9,12,24,33,34,49,61,81,86,102,113,117,142,**162**,200
I_8:2.81/2.60/2.61	$^2A_1/C_{2v}$	–1009.11922/1.05			15,17,24,33,44,56,71,73,78,124,**133**,148,187,196
I_9:2.85/2.70/2.89	$^4B_{1u}/D_{2h}$	–1009.08882/1.88			11,24,27,29,32,50,66,90,97,111,124,135,**143**,179

The optimized structures of the Au_7Cu cluster are displayed in Fig. 6, and their properties are given in Table 7. The lowest energy structure for Au_7Cu cluster is clearly of a tetra-edge-capped rhombus (I_1). This geometry was also the most stable one for the Au_8 cluster.[18] Isomer I_2 has a 3D structure with the Cu atom occupying the centre, which is 0.17 eV higher in energy than isomer I_1. Isomers I_4 and I_6 may originate from one Cu atom substitution in the capped hexagon structure of Au_8.[18] Isomers I_3 and I_5 are planar configurations, which might be well described as perturbations to the extended W form of the Au_6Cu cluster by the one Au or Cu atom. The values of binding energy per atom for these isomers of Au_7Cu lie in a range of 1.60–1.23 eV. As for the ground state structure displayed in Ref. [21], it is not found in our optimizations.

Table 7. Properties of the Au_7Cu cluster: geometry, molecular state and point group, relative energy, binding energy per atom (E_b) and dipole moment for isomer I_1, and vibrational frequency (bold figures are frequencies of the most IR-intense mode).

geometry $r_1/r_2\ldots$/Å	state/group	total energy (arb. units)/I_1 (eV)	E_b/eV	dipole moment /Debye	frequency/cm^{-1}
I_1:2.54/2.75/2.69/	$^1A_1/C_{2v}$	–1144.66465/0.00	1.60	2.6349	3,22,32,36,38,47,56,59,80,85, 100,102,131,133,**162**,172,212
I_2:2.73/2.61/2.53	$^1A_1/C_{2v}$	-1144.65828/0.17			12,14,19,20,50,51,54,58,68,75, 78,85,99,101,123,154,221,**222**
I_3:2.79/2.71/2.58	$^1A_1/C_{2v}$	–1144.64225/0.61			10,20,33,37,38,45,59,61,81,92, 98,108,124,136,**151**,178,212
I_4:2.56/2.76/2.70	$^1A_1/C_{2v}$	–1144.63622/0.77			5,21,31,34,36,39,44,46,57,66, 89,90,114,118,119,142,**152**,200
I_5:2.73/2.52/2.77	$^3B_2/C_{2v}$	-1144.61028/1.48			6,11,27,31,34,38,39,56,66,89, 91,105,114,140,142,**149**,211
I_6:2.79/2.73/2.72	$^5A_1/C_{2v}$	–1144.55505/2.98			12,19,28,29,32,37,47,49,75,82, 92,105,117,130,**137**,147,183

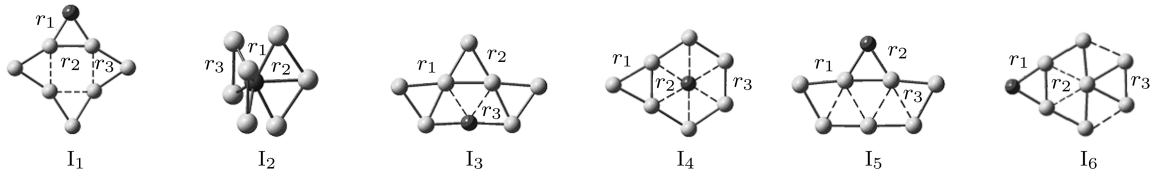


Fig. 6. Stable structures of Au_7Cu, where Cu atoms are denoted as dark spheres. The values of distance r_i are given in Table 7.

4. Stability trend

In this section, the stability trends of the Au_nCu (n = 1–7) clusters for ground-state structures are analysed in terms of the energy gaps between the highest occupied molecular orbital (HOMO) and lowest unoccupied molecular orbital (LUMO), the atomic averaged binding energies, the second-order difference of energies, and the fragmentation energies.

The energy gap (E_g) between the HOMO and LUMO is an important quality to characterise the cluster chemical stability. It is well known that the DFT typically underestimates the HOMO–LUMO gap. However, it still makes sense to examine the tendency of HOMO–LUMO gap among Au_nCu clusters. A large energy gap corresponds to higher stability. The calculated HOMO–LUMO gaps for the ground states of Au_nCu (n = 1–7) clusters are presented in Fig. 7. It can be seen from Fig. 7 that two clusters, AuCu and Au_5Cu, each have a particularly large energy gap. In other words, the AuCu and Au_5Cu clusters presumably have higher chemical stabilities.

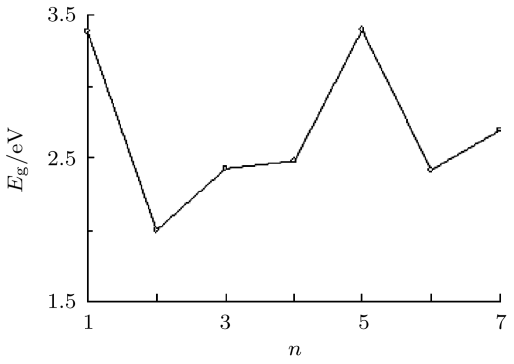


Fig. 7. HOMO–LUMO gaps of the ground states of the Au_nCu (n = 1–7) clusters.

The values of atomic averaged binding energy E_b of the Au_nCu clusters are defined as

$$E_b[Au_nCu] = (nE[Au] + E[Cu] - E[Au_nCu])/(n+1), \quad (1)$$

where E[Au], E[Cu], and E[Au_nCu] are the energies of an Au atom, a Cu atom, and the Au_nCu cluster. The variation of calculated binding energy per atom (E_b) of the most stable structure for each cluster with cluster size is shown in Fig. 8. As can be seen from the plot, binding energy per atom increases with cluster size and has a maximum value at Au_5Cu. This indicates that the ground-state Au_5Cu is more stable than its neighbours. The increase of E_b[Au_nCu] with n indicates the greater stability as the cluster grows in size. This may be due to the fact that with cluster size increasing, the average number of the nearest neighbours increases, which promotes the greater average number of interactions per atom.

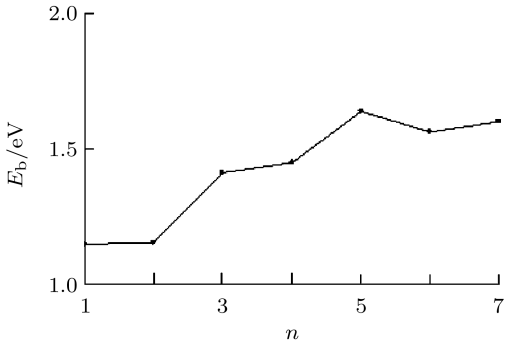


Fig. 8. Binding energy per atom of isomer vs. n for Au_nCu cluster.

In cluster physics, the second-order difference in energy ($\Delta^2 E$) is an extremely sensitive quantity that reflects the relative stability of the clusters.[18] For the ground-state Au_nCu clusters, it can be calculated as

$$\Delta^2 E[Au_nCu] = 2E_b[Au_nCu] - E_b[Au_{n+1}Cu] - E_b[Au_{n-1}Cu]. \quad (2)$$

Figure 9 shows the variation of the second differential of binding energy per atom with cluster size n. The plot shows that an odd–even oscillations with the even numbered clusters have larger $\Delta^2 E$ values. This indicates that odd-number Au_nCu clusters are more stable

than the neighbouring even-numbered ones. Among all the minimum energy structures, triangular Au_5Cu has the largest $\Delta^2 E$ value of 0.27 eV/atom. Consequently, it can be deduced that the Au_5Cu cluster possesses relatively high stability.

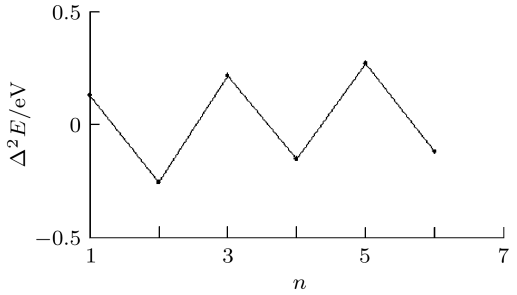


Fig. 9. Size dependence of the second-order energy difference for the ground-state Au_nCu cluster.

The relative stability of the ground-state Au_nCu cluster can also be discussed by examining fragmentation energy, which involves a fragmentation channel, $Au_nCu \rightarrow Au_{n-1}Cu + Au$. In this case, the fragmentation energy (ΔE) can be estimated as follows:

$$\Delta E(Au_nCu) = E(Au_{n-1}Cu) + E(Au) - E(Au_nCu), \quad (3)$$

where E is the energy of the ground-state cluster or atom. Figure 10 shows ΔE of the ground-state Au_nCu clusters, which oscillates as the cluster size increases and indicates that the clusters with even number of atoms are more stable than the clusters with odd number of atoms. The fragmentation energy for the most stable Au_5Cu cluster has a highest value of 2.57 eV, indicating high stability of Au_5Cu cluster. This is also in line with the above analysis based on E_b and $\Delta^2 E$ of the Au_nCu clusters.

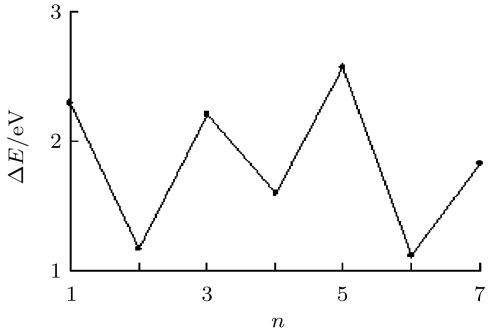


Fig. 10. Size dependence of fragmentation energy (ΔE) of the ground-state Au_nCu clusters with the loss of an Au atom.

5. Summary

The possible low-lying isomers and stability trend of the Au_nCu, n = 1–7, clusters have been investigated in this work using the density functional method B3LYP with relativistic effective core potentials (RECP) and LANL2DZ basis set. The geometric optimizations indicate that the ground-state Au_nCu clusters possess planar structures for n = 1–7, which are very similar to the pure Au_n clusters. The analyses of HOMO–LUMO gaps, fragmentation energies, and second-order difference of energies show that odd-number Au_nCu clusters are more stable than the neighbouring even-number ones, and stabilities at $n = 5$ for the ground-state Au_nCu clusters are enhanced. We also found from the averaged binding energies that the Au_5Cu cluster have high stability.

References

[1] Die D, Kuang X Y, Guo J J and Zheng B X 2009 *J. Mol. Struct. (Theochem)* **902** 54

[2] Mao H P, Wang H Y and Sheng Y 2008 *Chin. Phys.* B **17** 2110

[3] Hao F, Zhao Y, Li X and Liu F 2007 *J. Mol. Struct. Theochem.* **807** 153

[4] Wu Z J 2005 *Chem. Phys. Lett.* **406** 24

[5] Koyasu K, Naono Y, Akutsu M, Mitsui M and Nakajima A 2006 *Chem. Phys. Lett.* **422** 62

[6] Xu Y, Xu C, Zhou T and Cheng C 2009 *J. Mol. Struct. (Theochem.)* **893** 88

[7] Sinfelt J H 1983 *Bimetallic Catalysis: Discoveries Concepts and Applications* (New York: Wiley) p367

[8] Zhao Y, Jing X and Su W 2002 *J. Mol. Struct. (Theochem.)* **587** 43

[9] Liu F L, Zhao Y F, Li X Y and Hao F Y 2007 *J. Mol. Struct. (Theochem.)* **809** 189

[10] Li X, Kuznetsov A E, Zhang H F, Boldyrev A I and Wang L S 2001 *Science* **291** 859

[11] Mao H P, Wang H Y, Zhu Z H and Tang Y J 2006 *Acta Phys. Sin.* **55** 4542 (in Chinese)

[12] Yuan D W, Wang Y and Zeng Z 2005 *J. Chem. Phys.* **122** 114310

[13] Deschpande M, Dhavale A, Zope R R, Chacko C and Kanhere D G 2000 *Phys. Rev.* A **62** 063202

[14] Baruah T, Blundell S A and Zope R R 2001 *Phys. Rev.* A **64** 043202

[15] Deshpande M D, Kanhere D G, Vasiliev I and Martin R M 2003 *Phys. Rev.* B **68** 035428

[16] Guo J J, Yang J X, Die D, Yu G F and Jiang G 2005 *Acta Phys. Sin.* **54** 3571 (in Chinese)

[17] Wang F and Liu W 2005 *Chem. Phys.* **311** 63

[18] Deka A and Deka R C 2008 *J. Mol. Struct. (Theochem.)* **870** 83

[19] Koszinowski K, Schröder D and Schwarz H 2003 *Chem. Phys. Chem.* **4** 1233

[20] Häkkinen H, Abbet S, Sanchez A, Heiz U, Landman U and Angew 2003 *Chem. Int. Ed.* **42** 1297

[21] Wang H Y, Li X B, Tang Y J, King R B and Schaefer H F 2007 *Chin. Phys.* **16** 1660

[22] Zhao L X, Feng X J, Cao T T, Liang X and Luo Y H 2009 *Chin. Phys.* B **18** 2709

[23] Bouwen W, Vanhoutte F, Despa F, Bouckaert S, Neukermans S, Kuhn L T, Weidele H, Lievens P and Silverans R E 1999 *Chem. Phys. Lett.* **314** 227

[24] Heinebrodt M, Malinowski N, Tast F, Branz W, Billas I M L and Martin T P 1999 *J. Chem. Phys.* **110** 9915

[25] Becke A D 1988 *Phys. Rev.* A **38** 3098

[26] Lee C, Yang W and Parr R G 1988 *Phys. Rev.* B **37** 785

[27] Wadt W R and Hay P J 1985 *J. Chem. Phys.* **82** 284

[28] Frisch M J, Trucks G W, Schlegel H B *et al.* 2003 *Gaussian* 03 (Pittsburgh PA: Gaussian Inc.)

[29] Morse M D 1986 *Chem. Rev.* **86** 1049

[30] Bishea G A and Morse M D 1991 *J. Chem. Phys.* **91** 5646

[31] Bishea G A, Pinegar J C and Morse M D 1995 *J. Chem. Phys.* **95** 5630